Research Square

Preprints are preliminary reports that have not undergone peer review.
They should not be considered conclusive, used to inform clinical practice,
or referenced by the media as validated information.

Dielectric relaxation in amorphous and crystalline Sb2Te3 thin films

Aleksei Kononov (kononov_aa@icloud.com)
The Herzen State Pedagogical University of Russia https://orcid.org/0000-0002-5553-3782
Rene Alejandro Castro
Herzen State Pedagogical University of Russia: Rossijskij gosudarstvennyj pedagogiceskij universitet imeni A I Gercena
Yuta Saito
National Institute of Advanced Industrial Science and Technology Tsukuba Center: Tokai Daigaku Kaiyo Gakubu Daigakuin Kaiyogaku Kenkyuka
Paul Fons
Keio University Faculty of Science and Technology Graduate School of Science and Technology: Keio Gijuku Daigaku Rikogakubu Daigakuin Rikogaku Kenkyuka
Gennady Bordovsky
Herzen State Pedagogical University of Russia: Rossijskij gosudarstvennyj pedagogiceskij universitet imeni A I Gercena
Nadezhda Anisimova
Herzen State Pedagogical University of Russia: Rossijskij gosudarstvennyj pedagogiceskij universitet imeni A I Gercena
Alexandr Kolobov
Herzen State Pedagogical University of Russia: Rossijskij gosudarstvennyj pedagogiceskij universitet imeni A I Gercena

Research Article

Keywords: phase-change alloys, van der Waals solids, 3D-2D transformation, dielectric spectroscopy

Posted Date: February 15th, 2021

DOI: https://doi.org/10.21203/rs.3.rs-226390/v1

License: This work is licensed under a Creative Commons Attribution 4.0 International License.
Read Full License

A. A. Kononov[1], R. A. Castro[1], Y. Saito[2], P. Fons[2, 3], G. A. Bordovsky[1], N. I. Anisimova[1] and A. V. Kolobov[1,2]

Dielectric relaxation in amorphous and crystalline Sb_2Te_3 thin films

[1]Herzen State Pedagogical University of Russia, Department of Physical Electronics, St. Petersburg, Russia
[2]National Institute of Advanced Industrial Science & Technology, Device Technology Research Institute, Tsukuba, Japan
[3]Faculty of Science and Technology, Keio University, 3-14-1 Hiyoshi, Kohoku-ku, Yokohama, Kanagawa 223-8522, Japan

E-mail: kononov_aa@icloud.com (A.A. Kononov)
A. A. Kononov ORCID: 0000-0002-5553-3782
R. A. Castro ORCID: 0000-0002-1902-5801
Y. Saito ORCID: 0000-0002-9576-1560
P. Fons ORCID: 0000-0002-7820-1924
G. A. Bordovsky ORCID: 0000-0002-8520-6758
N. I. Anisimova ORCID: 0000-0003-2150-9677
A. V. Kolobov ORCID: 0000-0002-8125-1172

Abstract

Sb_2Te_3 is an end-point of the GeTe-Sb_2Te_3 quasibinary tie-line that represents phase-change alloys widely used in optical and non-volatile phase-change memory devices. In the crystalline form it is also a prototypical topological insulator with a layered structure where covalently bonded quintuple layers are held together by weak van der Waals forces. One of the ways to fabricate a crystalline phase is solid-state crystallisation of an amorphous film, whereby the three-dimensional (3D) structure relaxes to the two-dimensional (2D) crystalline phase. The mechanism of the 3D-2D transformation remains unclear. In this work, we performed a study of relaxation processes in thin Sb_2Te_3 films in both amorphous and crystalline phases. We found that both phases possess two kinds of relaxators (type I and type II), where the type I fragments are identical in the two phases, while the relaxation of type II fragments are shifted to lower temperature in the amorphous phases. The activation energies of the associated relaxation processes and the values of the Havriliak-Negami parameters were determined. The differences between the relaxation processes in the two phases are discussed. The obtained result will contribute to better understanding of the 3D-2D transformation during the crystallisation of van der Waals solids.

Keywords: phase-change alloys, van der Waals solids, 3D-2D transformation, dielectric spectroscopy

Declarations

Funding

The reported study was performed within a Russia-Japan joint project funded by the Russian foundation for Basic Research (project number 20-52-50012) and the Japan Society for the Promotion of Science (project number JPJSBP120204815).

Conflicts of interest/Competing interests (include appropriate disclosures)

The authors declare that they have no conflicts of interest.

Availability of data and material (data transparency)

The data that support the findings of this study are available from the corresponding author upon reasonable request.

Code availability (software application or custom code)

N/A

Relevance Summary

The present work reports on dielectric relaxation of amorphous and crystalline Sb_2Te_3 films. Sb_2Te_3 is of great topical interest as a prototypical topological insulator and an end-point of GeTe-Sb_2Te_3 phase-change alloys. In its crystalline form it is layered a van der Waals solid. The reported similarities and differences in relaxation processes in the two phases provide insights into 3D-2D transformation during the crytallisation process and are of significance for both the studied - technologically important - material and a wider class of van der Waals solids.

1. Introduction

Antimony telluride, Sb_2Te_3, is at the same time a narrow-gap semiconductor and a topological insulator. Due to its properties Sb_2Te_3 has wide range of industrial applications in thermoelectric devices such as thermal sensors [1] and micro-coolers [2] and in laser fabrication [3]. It is also an end-point of the GeTe-Sb_2Te_3 quasi-binary alloys successfully used in optical and nonvolatile electronic memory devices [4, 5]. Sb_2Te_3 belongs to the class of layered van der Waals solids, where covalently bonded quintuple layers with the Te-Sb-Te-Sb-Te stacking sequence are held together by weak van der Waals interactions. Various methods have been used to fabricate antimony telluride thin films: thermal evaporation [6], electrochemical atomic layer epitaxy [7], sputtering [8], electrochemical method [9], flash evaporation [10], metalorganic chemical vapor deposition [11] and molecular-beam epitaxy [12].

While the structure and electronic properties of Sb_2Te_3 have been thoroughly investigated, studies of its dielectric properties have been rather limited. The dielectric properties of thermally evaporated Sb_2Te_3 thin films have been investigated in [13, 14] but to date there have been no reports on comparative studies of the amorphous and crystalline phases. Such a study would foster a significant interest because amorphous film possesses a three-dimensional (3D) structure, while the dimensionality is changed to 2D in the crystalline phase. Recently, 2D materials have become a topic of great interest and one potential fabrication technique is solid state crystallization from the amorphous phase [15]. In the present work, Sb_2Te_3 films obtained by magnetron sputtering were studied, since this method allows growth of homogeneous films.

One of the methods that allow the study of the structural and electrophysical properties of materials is dielectric spectroscopy. The technique allows the monitoring of the polarization of a material over a wide range of frequencies and temperatures; the obtained data make it possible to calculate the activation energy of relaxation processes and the dipole relaxation time. The purpose of the present work was to carry out a comparative investigation of the dielectric properties of amorphous and crystalline Sb_2Te_3 films.

2. Experimental

Thin antimony telluride films, 80 nanometers thick, were obtained by RF magnetron sputtering on a silicon substrate at room temperature [16]. The dielectric spectra were measured with a wide-band dielectric spectrometer "Concept-81" (Novocontrol Technologies). Gold plated electrodes manufactured by Novocontrol Technologies GmbH were used to contact the sample. In this study, the dielectric properties were investigated over the frequency range f = 1 Hz – 1 MHz at T = -60 – 100°C. The frequency dependences of the dielectric constant ε' the dielectric loss factor ε'' and the dielectric loss tangent $tg\delta$ were obtained for both amorphous and crystalline Sb_2Te_3 films.

3. Results and discussion

The frequency dependence of the normalized dielectric constant ε′ for amorphous and crystalline Sb_2Te_3 films at room temperature is shown in figure 1 (left and right panels, respectively). It can be seen that ε′ decreases with increasing frequency, while the curves change their slope several times. This result indicates the presence of several types of relaxators in the material, which are involved in the polarization process at different frequencies. At low frequencies ($f < 10^1$ Hz), the dielectric constant reaches its maximum and goes to a plateau – the polarization saturates.

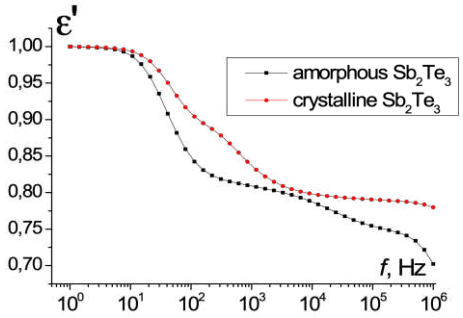

Fig. 1 The frequency dependence of the dielectric constant in normalized units at T = 20°C

Figures 2 and 3 present the temperature dependences of *tgδ* obtained for amorphous and crystalline Sb_2Te_3 films, respectively.

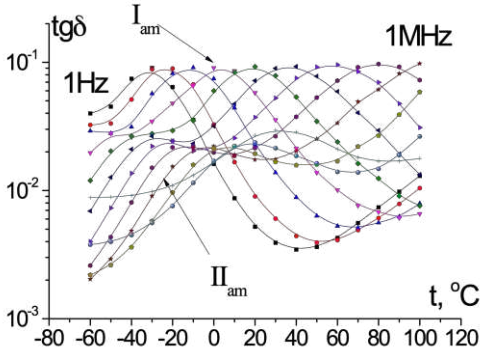

Fig. 2 Temperature dependences of *tg*δ for amorphous Sb_2Te_3

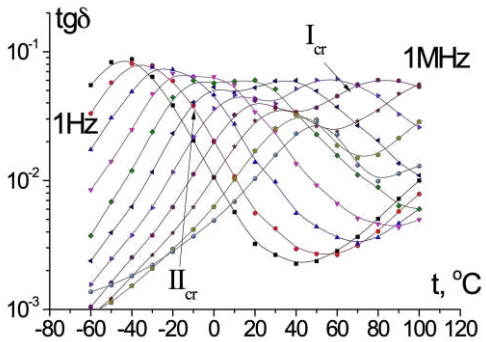

Fig. 3 Temperature dependences of *tg*δ for crystalline Sb_2Te_3

The temperature-frequency dependences of the dielectric loss tangent make it possible to detect the presence of relaxation processes in a material and allow one to estimate the parameters of the process and the degree of its symmetry/asymmetry relative to the maximum of the process. In the current case, figures 2 and 3 show two $tg\delta_{max}$ peaks, and, therefore, two polarization processes, which are indicated in the figures by the numbers I and II. Figures 4 and 5 show how the "humps" of the relaxation processes move to the high-frequency region with increasing temperature. This behavior is inherent to many semiconductors and is due to the increase in the mobility of kinetic units with increasing temperature.

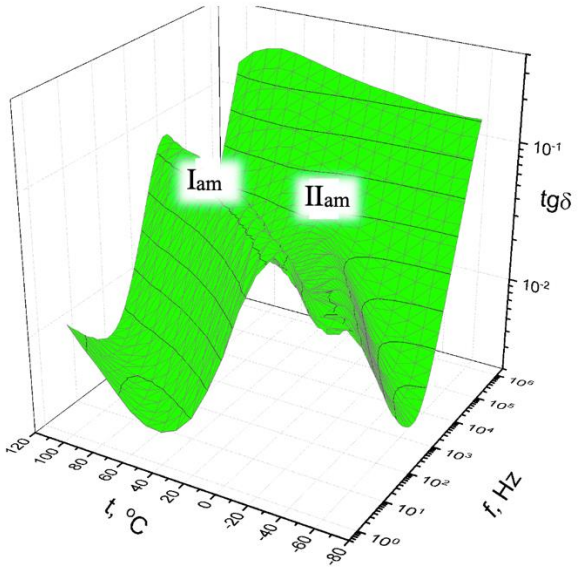

Fig. 4 3-D diagrams of *tg*δ for amorphous Sb_2Te_3

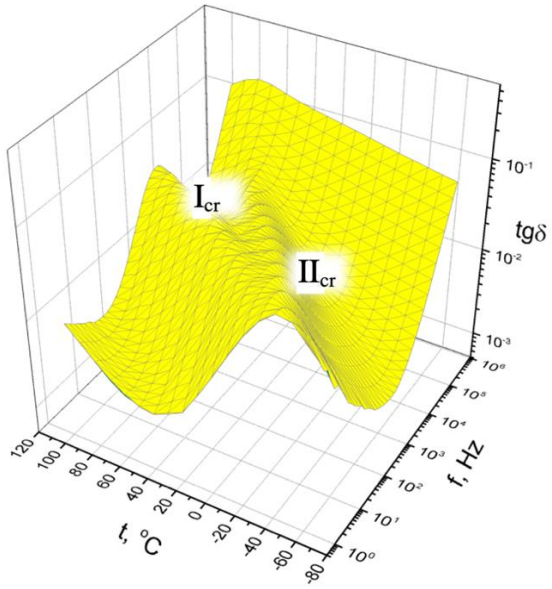

Fig. 5 3-D diagrams of *tg*δ for crystalline Sb_2Te_3

Figures 4 and 5 show that for amorphous and crystalline samples the curves corresponding to processes I are in the same frequency and temperature range.

The analysis of the dielectric spectra was performed by describing complex permittivity ε^* with the empirical Havriliak-Negami (HN) equation [17]:

$$\varepsilon^*(\omega) - \varepsilon_\infty = \sum_{k=1}^{n} \mathrm{Im}\left[\frac{\Delta\varepsilon_k}{\{1+(i\omega\tau_{HN_k})^{\alpha_k}\}^{\beta_k}}\right] \quad (1)$$

Here, $\varepsilon^* = \varepsilon'(\omega) - i\varepsilon''(\omega)$; $\omega = 2\pi f$; $\Delta\varepsilon = \varepsilon_0 - \varepsilon_\infty$ is the increment of dielectric permittivity ($\varepsilon_0 = \varepsilon'$ at $\omega \to 0$, $\varepsilon_\infty = \varepsilon'$ at $\omega \to \infty$); τ_{HN} is the characteristic time of the HN equation; α_{HN} and β_{HN} are calculated parameters corresponding to the widening and asymmetry of the relaxation time distribution, respectively.

The separation of the observed processes and the calculation of the corresponding parameters were carried out with the program WinFit by "Novocontrol Technologies". Examples of deconvolution of the dielectric spectrum according to equation (1) into two components (processes I and II) are shown in figure 6. It can be observed that the values of the dielectric loss factor ε''_{max} for the amorphous sample are larger than the corresponding crystalline values. One might have expected the opposite result based on the available literature data on phase-change [18], however, we note that the frequencies used in our experiments are many orders of magnitude lower than optical frequencies. We further note that even in the optical range there are regions where the values n and k for the amorphous phase are higher than those for the crystalline phase. We believe that the observed higher values of ε'' are due to an increase in the degree of disorder, which increases the response to an external electric field and, consequently, to an increase in dielectric losses.

The most probable relaxation time τ_{max} corresponding to the position of ε''_{max} on the frequency dependence $\varepsilon'' = \varphi(f)$ has been calculated as [19]:

$$\tau_{\max} = \tau_{HN}\left[\frac{\sin\left(\frac{\pi\alpha_{HN}\beta_{HN}}{2(\beta_{HN}+1)}\right)}{\sin\left(\frac{\pi\alpha_{HN}}{2(\beta_{HN}+1)}\right)}\right]^{1/\alpha_{HN}} \quad (2)$$

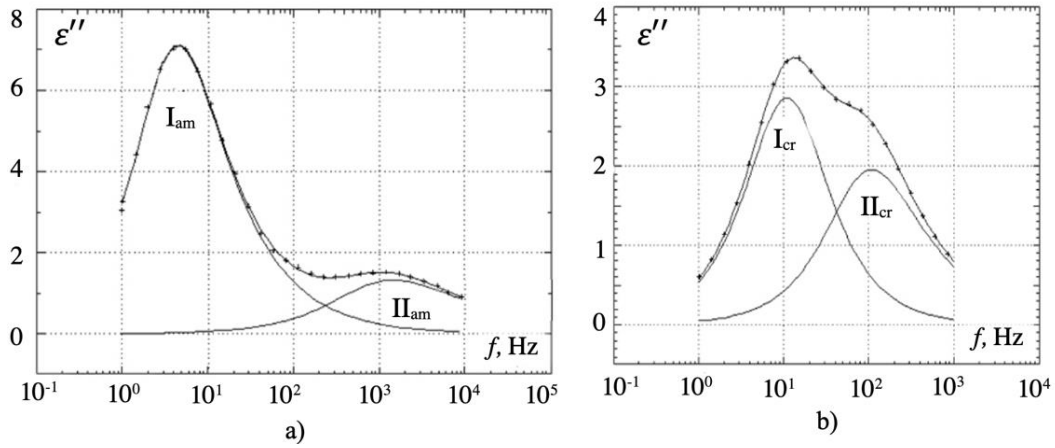

Fig. 6 The deconvolution of the dielectric spectrum at t = 0 °C by the HN equation into two components (processes I and II). Amorphous Sb_2Te_3 – (a), crystalline Sb_2Te_3 – (b)

The temperature dependences of relaxation time are shown in Arrhenius coordinates in figure 7.

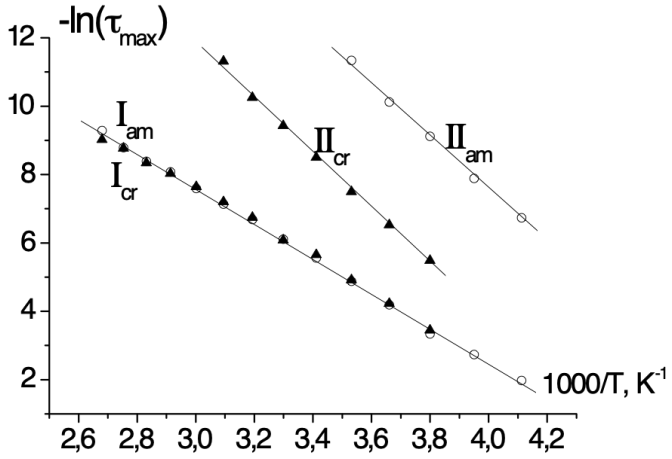

Fig. 7 Dependences of $-\log\tau_{max}$ on inverse temperature over the range of processes I and II. Points are calculations of τ_{max} according to the HN equation (1). II_{am} and I_{am} – dependences for amorphous Sb_2Te_3, I_{cr} and II_{cr} – for crystalline Sb_2Te_3.

Figure 7 shows that processes I for amorphous and crystalline samples are similar – the dependences of the relaxation time are the nearly identical.

The temperature dependences of the relaxation time, $-log\tau_{max}=\varphi(1/T)$, is linear and can be described by the Arrhenius equation:

$$\tau(T)_{max} = \tau_0 \exp({}^{E_a}/_{RT}), \quad (3)$$

E_a — activation energy.

The shape of the curves on the dependence $-log\tau_{max}=\varphi(1/T)$ allows determination of the type of polarization observed in the material. There are four polarization mechanisms that contribute to the relative permittivity of a material: electronic polarization, ionic polarization, dipolar polarization and interfacial polarization. Dipolar polarization and interfacial polarization are dielectric relaxation processes, while ionic and electronic polarization show resonances or oscillatory behavior [20]. The detected relaxation processes (figure 6) observed in the intermediate frequency range ($f = 10^0$ Hz – 10^4 Hz), have linear dependences on the relaxation times (figure 7), the maxima of the loss factor in figures 2 and 3 shifts towards high frequencies with increasing temperature - all these facts indicate that the processes under study are dipole relaxation processes. This conclusion is consistent with the results of [13], who also discovered the existence of dipole-relaxation polarization in the same frequency range.

The activation energies for processes I and II were calculated according equation (3) and are presented in Table 1.

Table 1. Activation energy of I and II processes.

$E_a(I_{am})$, eV	$E_a(I_{cr})$, eV	$E_a(II_{am})$, eV	$E_a(II_{cr})$, eV
0.43±0.01	0.44±0.01	0.68±0.02	0.70±0.02

The values of the relaxation parameters of the HN equation for the Sb_2Te_3 samples at different temperatures are presented in Table 2.

Table 2. The value of the HN parameters of the Sb_2Te_3 samples. The error of the calculated values does not exceed 5%.

T, K	I				II			
	crystalline		**amorphous**		**crystalline**		**amorphous**	
	α	***β***	***α***	***β***	***α***	***β***	***α***	***β***
263	1	1	1	0.73	0.93	0.76	0.84	0.54
283	0.98	0.99	1	0.84	1	0.54	0.79	0.26
303	0.99	1	1	0.82	0. 78	0.79	-	-
323	0.98	1	1	0.78	0.89	0.28	-	-

The parameters α and β for prosses I_{cr} are equal to 1. Such parameter values satisfy the Debye dielectric dispersion equation for a symmetric distribution of relaxation times [21]:

$$\varepsilon^* = \frac{D(t)}{\varepsilon_0 E(t)} = \varepsilon_\infty + \frac{\varepsilon_s - \varepsilon_\infty}{1+i\omega\tau}. \quad (4)$$

Processes of this type are usually caused by the relaxation of a single type of dipoles in an alternating electric field. The above equation is not suitable for describing processes with wide distribution of interactions. Such a complex behavior is characteristic of the non-Debye process I_{am} for which α = 1 and β ≠ 1. This process is described by the Cole-Davidson model [22]:

$$\varepsilon^* = \varepsilon_\infty + \frac{\varepsilon_0 - \varepsilon_\infty}{(1+i\omega\tau)^\beta}. \quad (5)$$

Thus, process I_{cr} is a typical relaxation process, which is caused by the relaxation of a single type of relaxators, which is explained by the periodicity of the crystal structure. Amorphous material retains only short-range order. Consequently, the accumulating disorder leads to a distribution of bind lengths and angles in the local structural fragments, which, when superimposed on each other, lead to an asymmetric distribution of relaxation times. However, as we see from Figure 7 and Table 2, these structural modifications do not lead to any significant changes in activation energy of the process I.

For process II of amorphous and crystalline Sb_2Te_3, the values of parameters are calculated to be $\alpha \neq 1$ and $\beta \neq 1$ (table 2). Such processes are described by the Havrilyak-Negami equation (equation 1). These processes are observed at higher frequencies ($f = 10^2$ Hz – 10^3 Hz), which suggests that they are caused by the movement of smaller relaxators than in the case of process I, whose concentration increases in the amorphous phase, causing to lower temperatures compared to process in the crystalline phase II_{cr} (figure 7).

We also note that while the stable structure of the crystalline phase is 2D layered, a metastable cubic phase with a large concentration of vacancies has also been reported [23] and it is natural to assume that the 3D cubic phase is closer to the 3D amorphous phase.

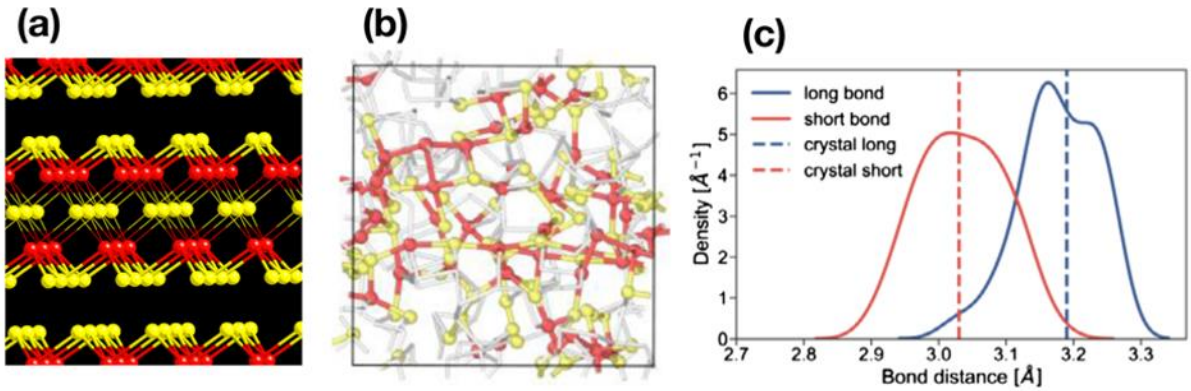

Fig. 8 Fragments of crystalline (a) and amorphous (b) Sb_2Te_3 structures. In both cases, linear fragments with alternating short and long Sb-Te bonds are clearly visible. The shorter and longer Sb-Te interatomic distances are also very similar in the two cases (panel c). Panels (b) and (c) are reproduced from [24] with permission from John Wiley and Sons.

In both cases, there are extended …Te-Sb-Te-Sb… fragments with multicenter hyperbonds (Fig. 8a,b). Such bonds are usually asymmetric, i. e. possess dipole moments [25]. It is also remarkable that the shorter and longer bond-lengths in such fragments are very similar in the amorphous and crystalline phases as can be seen from Fig. 8c [24]. We attribute the manifestation of process I to the presence of such, relatively heavy, fragments. We further notice that the local motifs in the 2D layered phase and in the 3D cubic phase are different, namely in the 2D phase octahedral fragments with central Sb atoms are surrounded by six Te atoms, while in the 3D phase there are defective octahedral sites with a smaller number of Te neighbors (cf. Fig. 5 of ref. 23). The larger number of the surrounding Te atoms may be the origin of heavier structural units and correspondingly higher temperatures in the crystalline phase.

4. Conclusion

We detected the existence of two relaxation processes in amorphous and crystalline Sb_2Te_3 films which is associated with the manifestation of dipole-relaxation polarization. In both cases there are two distinct relaxation processes. One of the processes is very similar in tow phases, while the other one shifts to lower temperatures in the amorphous phase. The observed processes are associated with similarities and differences in the local bonding in the

amorphous and crystalline phases. Process I is likely to be due to the presence of extended …Te-Sb-Te-Sb… fragments with multi-center bonds, while differences in the process II may be caused by the different number of Te neighbors in the Sb-centered octahedral fragments.

References

1. K. Rajasekar, L. Kungumadevi, A. Subbarayan, R. Sathyamoorthy, Ionics (2008) https://doi.org/10.1007/s11581-007-0146-3
2. L.M. Goncalves, C. Couto, P. Alpuim, D.M. Rowe, J.H. Correia, Sens Actuators (2006) https://doi.org/10.1016/j.sna.2005.10.014
3. J. Boguslawski, J. Sotor, G. Sobon, J. Tarka, J. Jagiello, W. Macherzynski, L. Lipinska, K. M. Abramski, Laser Phys. (2014) https://doi.org/10.1088/1054-660X/24/10/105111
4. T. Ohta, J. Optoelectron. Adv Mater. 3, 609 (2001)
5. J. Choe, Intel 3D XPoint memory die removed from Intel Optane™ PCM (phase change memory). (TechInsights Inc., 2017), https://www.techinsights.com/blog/intel-3d-xpoint-memory-die-removed-intel-optanetm-pcm-phase-change-memory
6. A.M. Farid, H.E. Atyia, N.A. Hegab, Vacuum (2005) https://doi.org/10.1016/j.vacuum.2005.05.003
7. J.Y. Yang, W. Zhu, X.H. Gao, X.A. Fan, S.Q. Bao, X.K. Duan, Electrochim Acta (2007) https://doi.org/10.1016/j.electacta.2006.09.045
8. A.E. Abken, O.J. Bartelt, Thin Solid Films (2002) https://doi.org/10.1016/S0040-6090(01)01527-9
9. İ.Y. Erdoğan, Ü. Demir, J. Electroanal Chem. (2009) https://doi.org/10.1016/j.jelechem.2009.06.010
10. H.S. Soliman, S. Yaghmour, H.G. Al-Solami, The European Physical Journal Applied Physics (2008) https://doi.org/10.1051/epjap:2008132
11. J.E. Boschker, J. Momand, V. Bragaglia, R. Wang, K. Perumal, A. Giussani, B. J. Kooi, H. Riechert, R. Calarco (2014) https://doi.org/10.1021/nl5011492
12. R. Venkatasubramanian, T. Colpitts, E. Watko, M. Lamvik, N. El-Masry, J. Cryst Growth (1997) https://doi.org/10.1016/S0022-0248(96)00656-2
13. K. Ulutas, D. Deger, S. Yakut, J Phys: Conf Ser. (2013) https://doi.org/10.1088/1742-6596/417/1/012040
14. A. M. Farid, H. E. Atyia, N. A. Hegab, Vacuum (2005) https://doi.org/10.1016/j.vacuum.2005.05.003
15. Y. Saito, S. Hatayama, Y. Shuang, P. Fons, A. V. Kolobov, Y. Sutou. Dimensional transformation of chemical bonding during crystallization in the layered chalcogenide material…. (will be published soon)
16. Y. Saito, P. Fons, A.V. Kolobov, K. Mitrofanov, K. Makino, J. Tominaga, S. Hatayama, Y. Sutou, M. Hase, J. Robertson, J Phys D Appl Phys. (2020) https://doi.org/10.1088/1361-6463/ab850b
17. S. Havriliak, S. Negami, Polymer (1967) https://doi.org/10.1016/0032-3861(67)90021-3
18. B.S. Lee, S.G. Bishop, Phase Change Materials: Science and Applications (2009) https://doi.org/10.1007/978-0-387-84874-7_9
19. R. Diaz-Calleja, Macromolecules (2000) https://doi.org/10.1021/ma991082i
20. C. Chen, P. Jost, H. Volker, M. Kaminski, M. Wirtssohn, U. Engelmann, M. Wuttig, Phys Rev B (2017) https://doi.org/10.1103/PhysRevB.95.094111
21. P. Debye, D. Ann, Physik 39, 789 (1912)
22. A.K. Jonsher, Dielectric Relaxation in Solids (Chelsea Dielectric Press, London, 1983)

23. Y. Zheng, M. Xia, et al., Nano Res. (2016) https://doi.org/10.1007/s12274-016-1221-8

24. T.H. Lee, S.R. Elliott, Adv. Mater. (2020) https://doi.org/10.1002/adma.202000340

25. F.C. Mocanu, K. Konstantinou, J. Mavračić, S.R. Elliott, Phys. Status Solidi RRL (2020) https://doi.org/10.1002/pssr.202000485

Figures

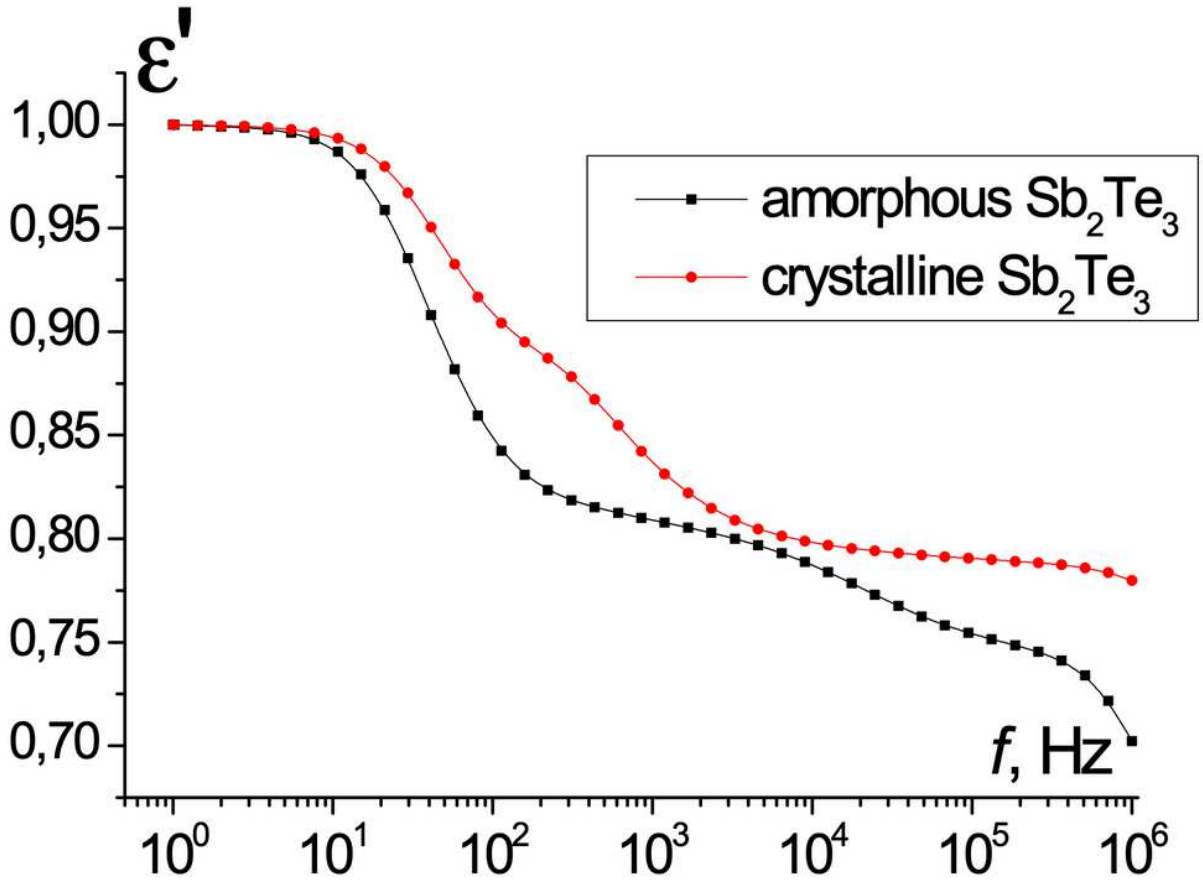

Figure 1

The frequency dependence of the dielectric constant in normalized units at T = 20ºC

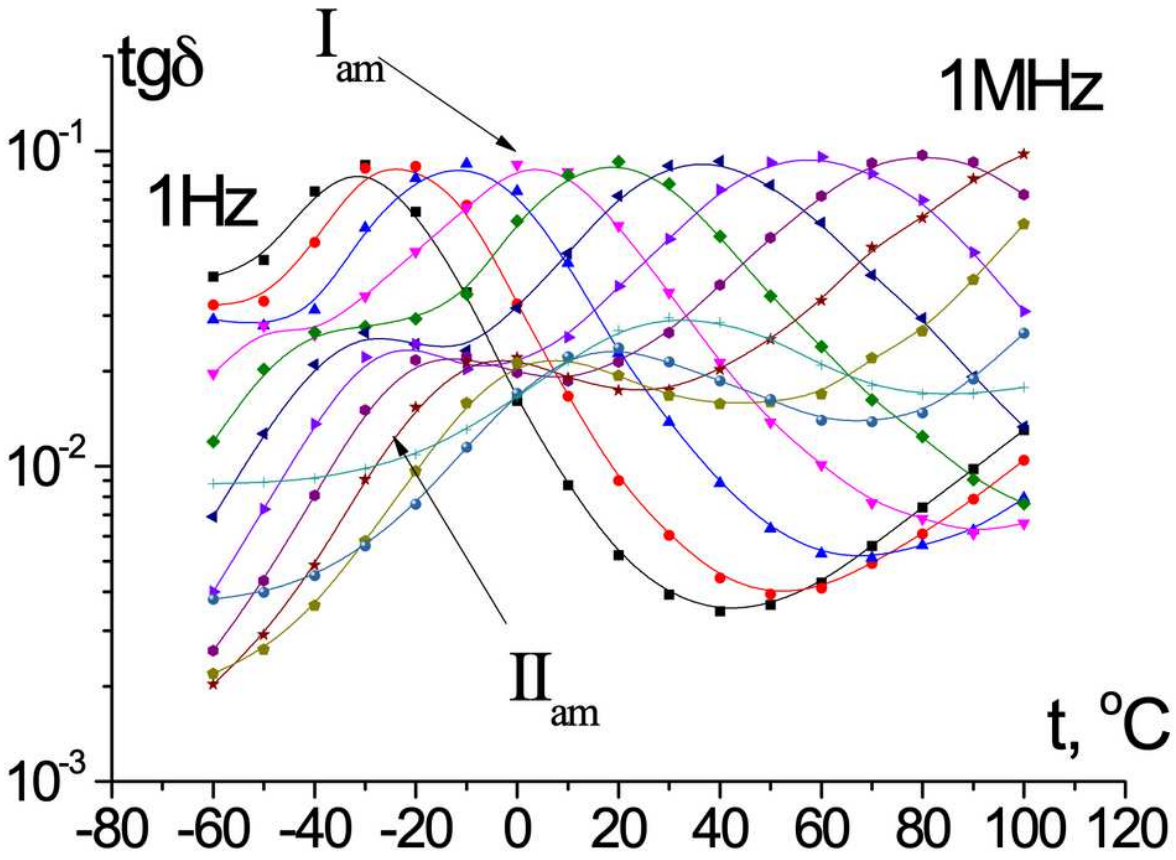

Figure 2

Temperature dependences of tgδ for amorphous Sb2Te3

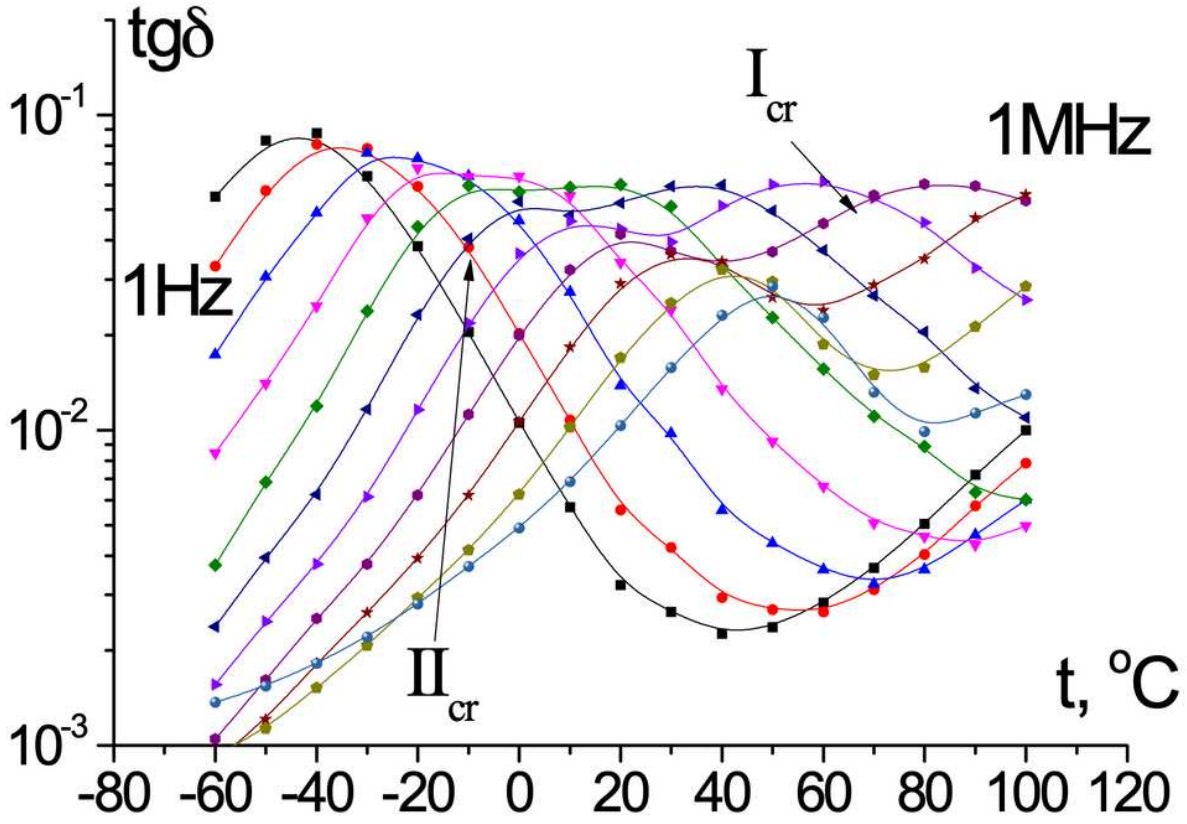

Figure 3

Temperature dependences of tgδ for crystalline Sb2Te3

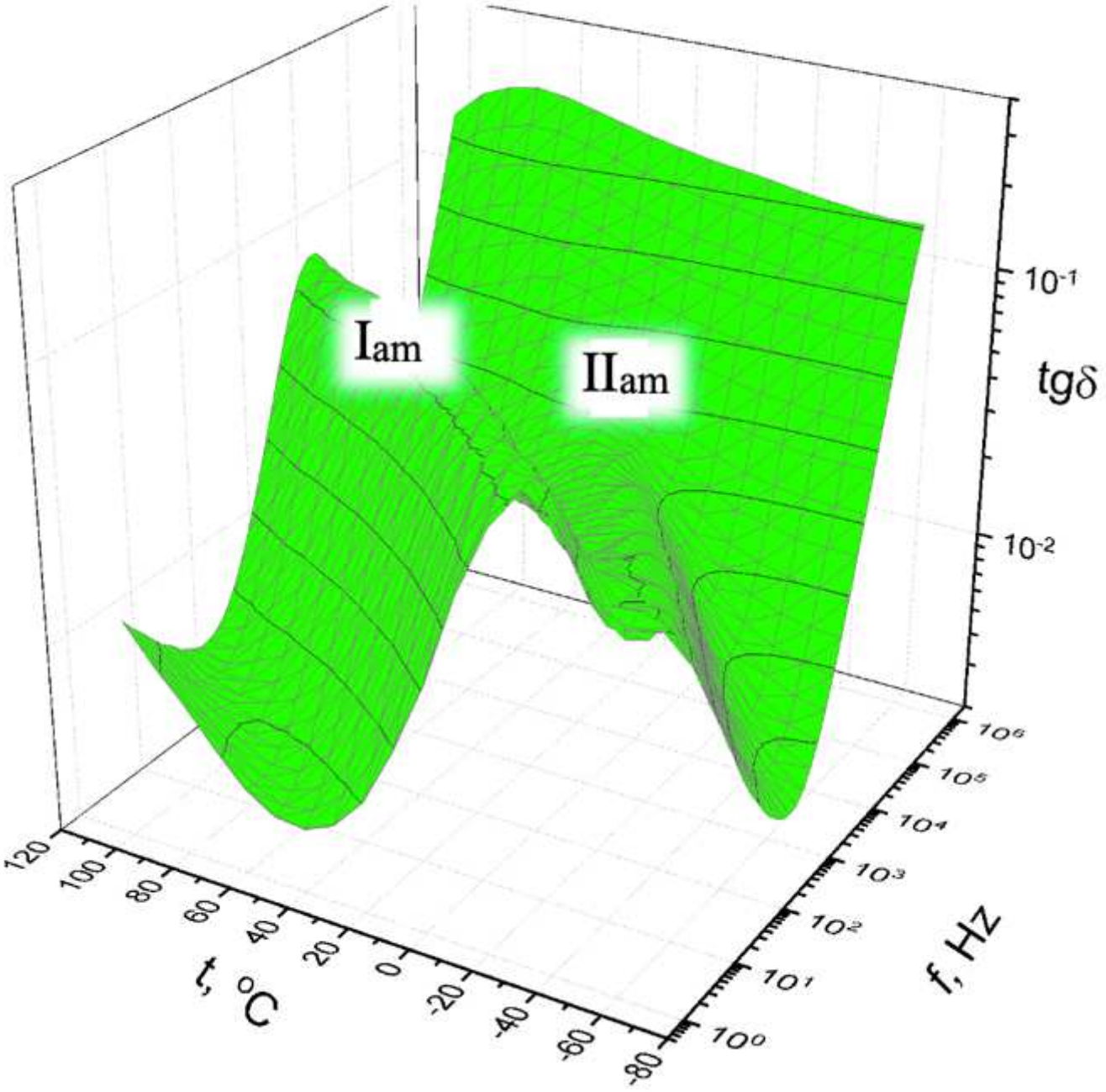

Figure 4

3-D diagrams of tgδ for amorphous Sb2Te3

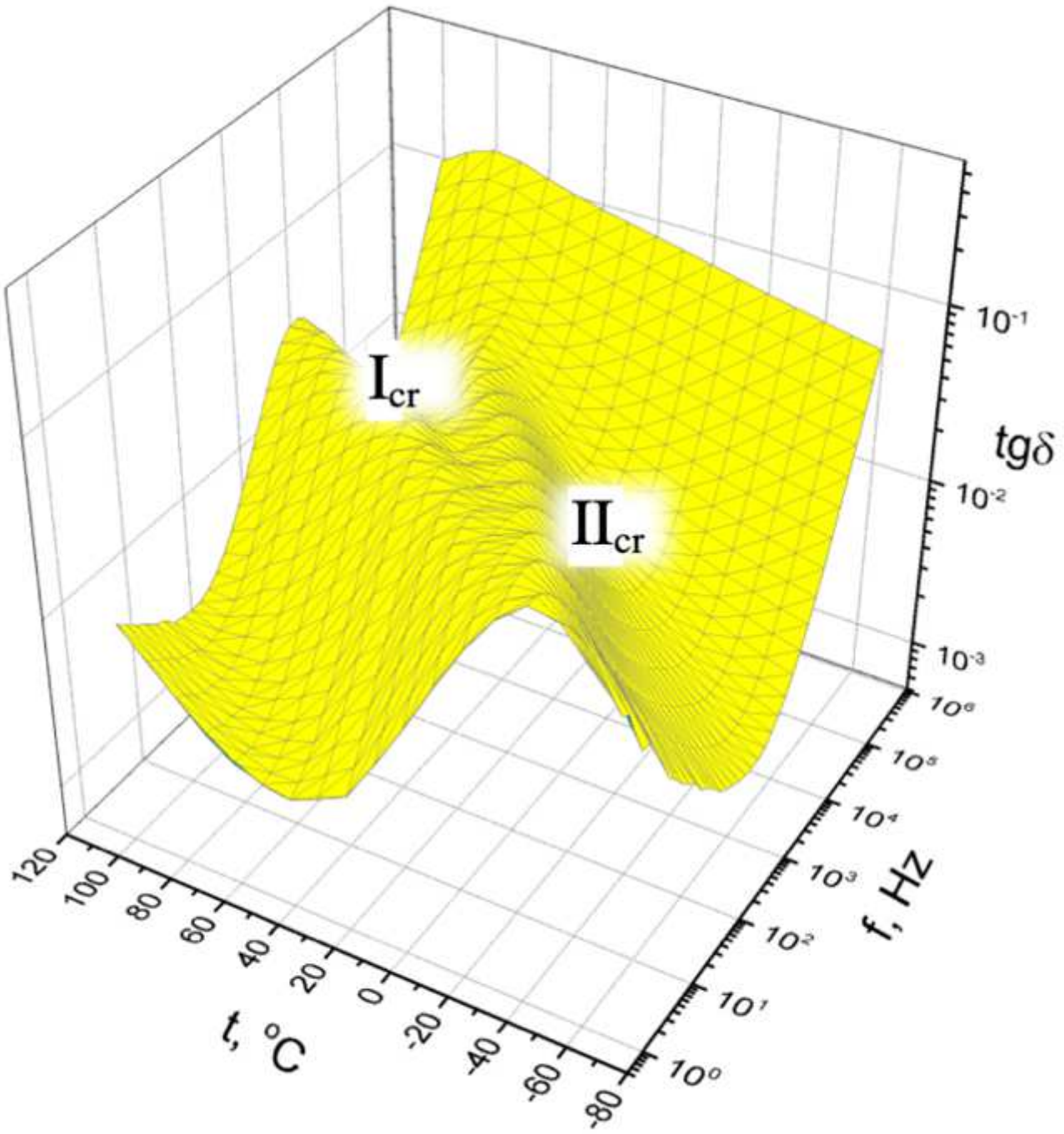

Figure 5

3-D diagrams of tgδ for crystalline Sb2Te3

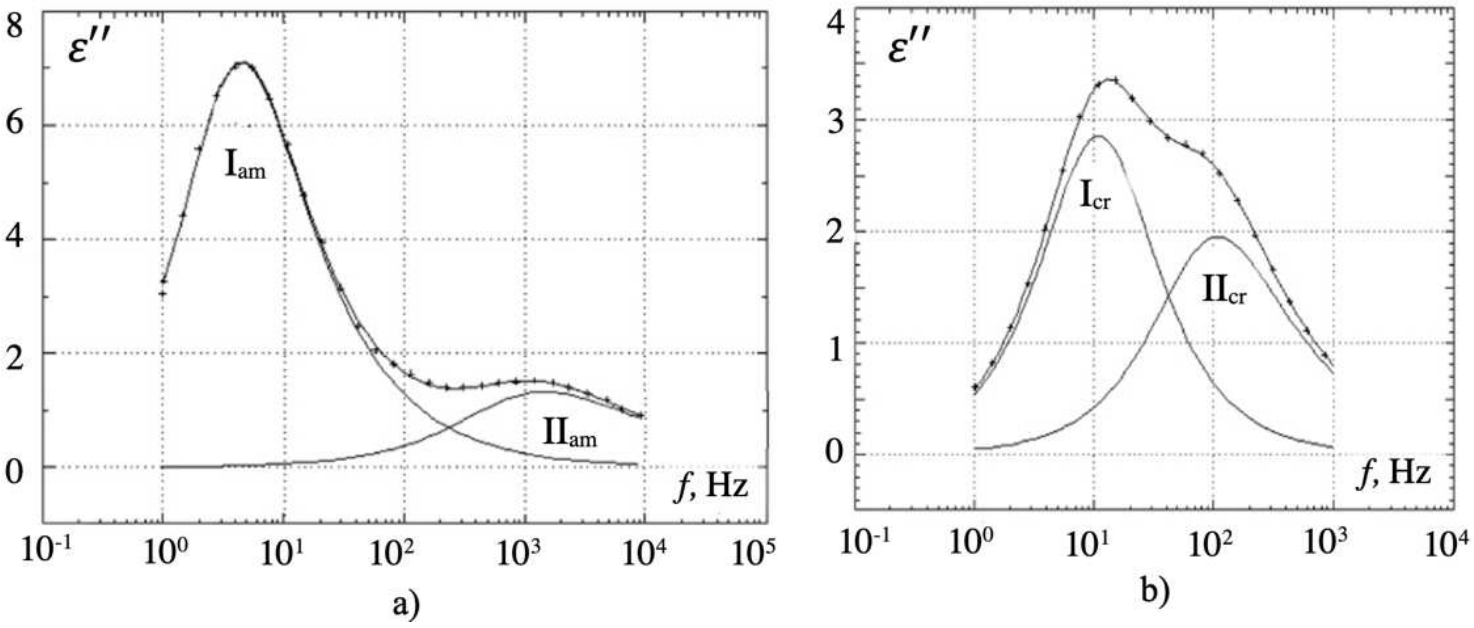

Figure 6

The deconvolution of the dielectric spectrum at t = 0 □ by the HN equation into two components (processes I and II). Amorphous Sb2Te3 – (a), crystalline Sb2Te3 – (b)

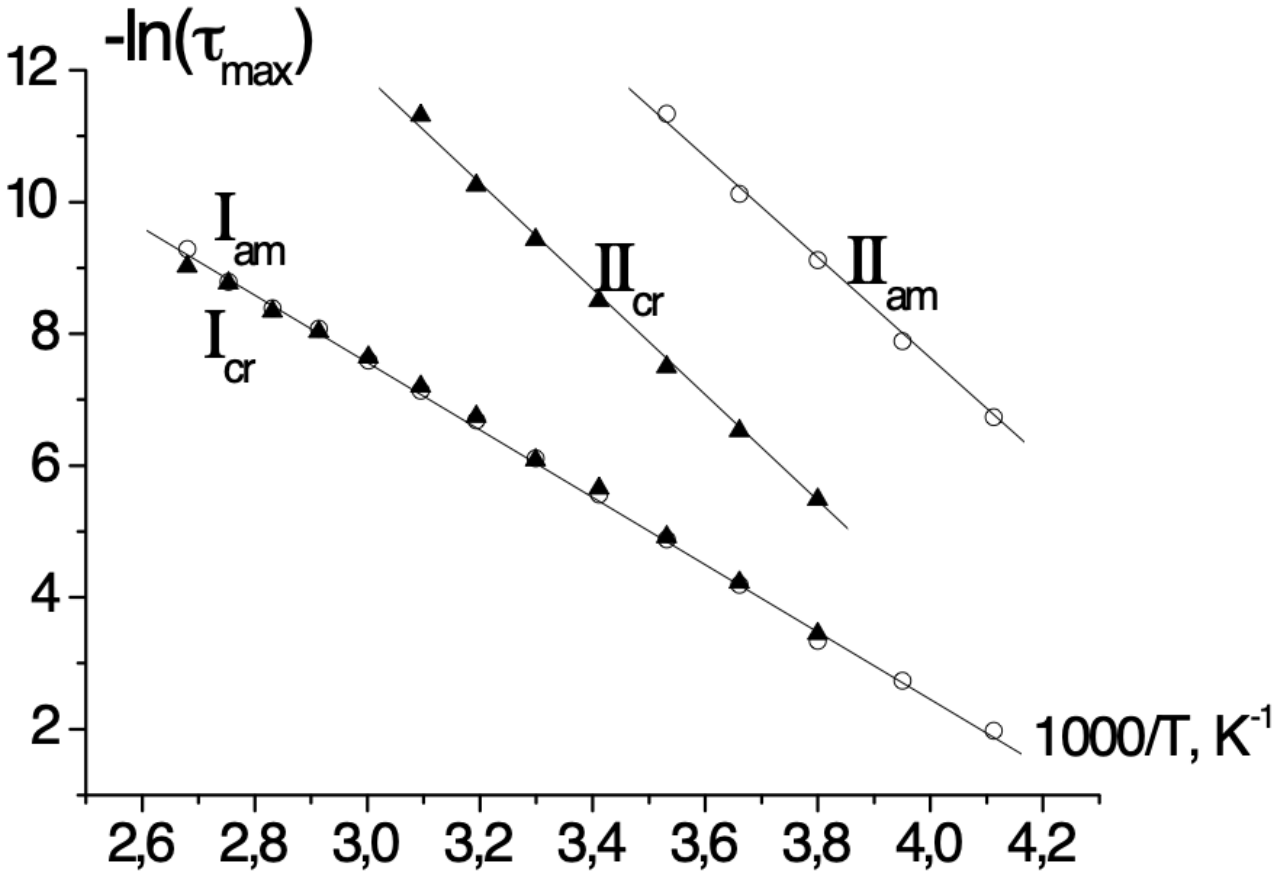

Figure 7

Dependences of −log□max on inverse temperature over the range of processes I and II. Points are calculations of □max according to the HN equation (1). IIam and Iam – dependences for amorphous Sb2Te3, Icr and IIcr – for crystalline Sb2Te3.

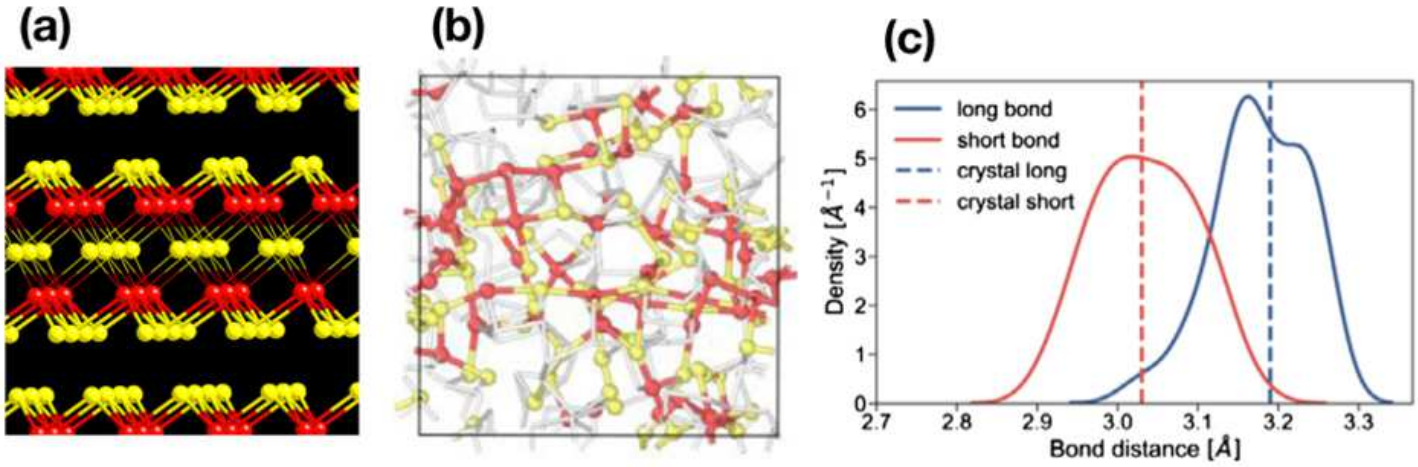

Figure 8

Fragments of crystalline (a) and amorphous (b) Sb2Te3 structures. In both cases, linear fragments with alternating short and long Sb-Te bonds are clearly visible. The shorter and longer Sb-Te interatomic distances are also very similar in the two cases (panel c). Panels (b) and (c) are reproduced from [24] with permission from John Wiley and Sons.